Vol 17 No 8, August 2008
1674-1056/2008/17(08)/2897-12

Chinese Physics B

© 2008 Chin. Phys. Soc.
and IOP Publishing Ltd

Peculiar features of the interaction potential between hydrogen and antihydrogen at intermediate separations*

Lee Teck-Ghee(李德义)[a)b)], Wong Cheuk-Yin(黄卓然)[a)c)], and Wang Lee-Shien(王礼贤)[d)]

[a)] *Physics Division, Oak Ridge National Laboratory, Oak Ridge, Tennessee* 37831, *USA*
[b)] *Department of Physics and Astronomy, University of Kentucky, Lexington, Kentucky* 40506, *USA*
[c)] *School of Physics & Optoelectronic Technology, Dalian University of Technology, Dalian* 116024, *China*
[d)] *Department of Physics, Harvey Mudd College, Claremont, California* 91711, *USA*

(Received 15 November 2007; revised manuscript received 27 December 2007)

This paper evaluates the interaction potential between a hydrogen and an antihydrogen using the second-order perturbation theory within the framework of the four-body system in a separable two-body basis. It finds that the H–$\bar{\text{H}}$ interaction potential possesses the peculiar features of a shallow local minimum located around interatomic separations of $r \sim 6$ a.u. and a barrier rising at $r \lesssim 5$ a.u.

Keywords: few-body problems, potential energy curve, perturbation theory, H–$\bar{\text{H}}$ interaction
PACC: 3000, 3180, 1120D

1. Introduction

Recent production of cold antihydrogen[1,2] has stimulated new theoretical and experimental interest in the interaction between H and $\bar{\text{H}}$. The four particles of the greater ($\text{e}^+\text{e}^-\text{p}\bar{\text{p}}$) system can be arranged in different ways leading to different types of states. On the one hand, there are states in the H–$\bar{\text{H}}$ family in which the e^+ and the e^- are not correlated but are orbiting around the $\bar{p}$ and the p respectively, with the H and the $\bar{\text{H}}$ appearing as composite particles. They are the lowest-energy states at large interatomic separations. On the other hand, there are states of the $Ps\text{p}\bar{\text{p}}$ family for which the e^+ and the e^- are highly correlated and orbit each other as in a positronium (Ps). The role of the $Ps\text{p}\bar{\text{p}}$ family and the H–$\bar{\text{H}}$ family is interchanged at short distances as the $\text{e}^+ - \text{e}^-$-correlated state of the $Ps\text{p}\bar{\text{p}}$ family becomes the state of the lowest energy, as indicated by the merging of the $V_{\rm var}(r)$ potential obtained by variational calculations with the $V_{Ps\text{p}\bar{\text{p}}}(r)$ potential obtained for the $Ps\text{p}\bar{\text{p}}$ configuration, at small interatomic separations (see Fig.4 below). Because the p and $\bar{p}$ can orbit around (and annihilate) each other under their mutual Coulomb and nuclear interactions,[3] the $Ps\text{p}\bar{\text{p}}$ family can be further bifurcated into subfamilies with a correlated or uncorrelated p-$\bar{p}$ pair. There are also states that are hybrid of different families.

If one can depict the orbiting of one particle relative to another particle as a 'dance pattern', then the dance patterns of the different families have distinctly different topological structures and connectivities. The distinct topological structures may allow them to retain some of their characteristics and stability. The mixing and the interplay between different families at different interatomic separations will provide a general idea on the 'genealogy' of the states. To be able to classify the greater ($\text{e}^+\text{e}^-\text{p}\bar{\text{p}}$) system into families, if at all possible, will bring us to a better understanding of the complexity of the spectrum that is associated with the complicated four-body problem, as well as to a better knowledge of the scattering between the H and the $\bar{\text{H}}$.

The H atom and the $\bar{\text{H}}$ atom can scatter from each other at various energies. The problem of the H–$\bar{\text{H}}$ scattering will require the knowledge of the interaction potential between the H and the $\bar{\text{H}}$ as composite particles. As the H and $\bar{\text{H}}$ may rearrange into other configurations and may annihilate at short distances, the scattering problem needs to be treated in general in a coupled-channel analysis involving different interaction potentials and transition matrix elements.[4]

*Project supported in part by the National Natural Science Foundation of China (Grant No 10575024), and in part by the Division of Nuclear Physics, Department of Energy (Grant No DE-AC05-00OR22725) managed by UT-Battelle, LLC.

For the elastic channel, one often takes the interaction potential to be the adiabatic potential obtained in a variational calculation for the lowest-energy state of the e^+ and the e^- in the Born–Oppenheimer potential.[4−10] The $e^+ - e^-$ correlation property of the lowest-energy adiabatic state will undergo a change as the interatomic separation changes. At large interatomic separations, the adiabatic lowest-energy state coincides with the incoming channel state of separated H and $\bar{H}$ atoms with uncorrelated e^- and e^+ orbiting around p and $\bar{p}$, respectively. At small interatomic separations, the variational calculations will naturally lead to the lowest-energy adiabatic state involving strong correlations between the e^+ and the e^- which differs from the elastic incoming channel by the presence of $e^+ - e^-$ correlations. An adiabatic approximation involves altering the nature of the underlying state from the incoming elastic channel with no $e^+ - e^-$ correlations to the other $e^+ - e^-$-correlated channel, as the interatomic separation decreases. A general consideration of the channel coupling however will contain both the incoming elastic channel and the $e^+ - e^-$-correlated channel in explicit coupling and transition. Depending on the collision energy, the dynamics of the scattering process will lead to the adiabatic case with strong $e^+ - e^-$ correlations at short separations in one limit of slow motion and large transition matrix elements. It will lead to the diabatic case with no $e^+ - e^-$ correlation of the atomic H and $\bar{H}$ in the other limit. To carry out the explicit channel coupling for the general case of an arbitrary energy, or to see the cross-over to either the adiabatic or the diabatic limit, it is necessary to obtain the interaction potential for the incoming entrance channel of a H and a $\bar{H}$.

In the present work, we focus our attention on the interaction potential for this incoming channel between the H and the $\bar{H}$ as composite particles, for which the e^- and the e^+ remain uncorrelated, orbiting around the p and $\bar{p}$ respectively, i.e. without the loss of the H and the $\bar{H}$ atomic identities. We are in effect trying to construct the interaction potential for one of the diabatic basis configurations in preparation for a general coupling of different diabatic basis states in a coupled-channel analysis. For brevity of nomenclature, we shall use the term 'the interaction potential' to refer to this potential between the composite particles H and $\bar{H}$, unless otherwise stated.

The interaction potential $V_{H\bar{H}}(r)$ between the composite H and the $\bar{H}$ can also be used to investigate possible H–$\bar{H}$ two-body molecular states of the H–$\bar{H}$ family, as the composite H and $\bar{H}$ atoms can form a bound system if their interaction potential is sufficiently attractive. These possible molecular two-body H–$\bar{H}$ states, if they exist, belong to the H–$\bar{H}$ family, a subset of the states of the greater four-body $(e^+e^-p\bar{p})$ system. One theoretical approach to study the lowest-energy state of the greater $(e^+e^-p\bar{p})$ system is to use the variational method equipped with either explicitly correlated Slater-type or Gaussian-type orbitals with $e^+ - e^-$ correlations. This method has provided a great wealth of information regarding the lowest-energy state of the four-body system.[5−9] As our interest is focused on the properties of possible two-body states of the composite H and $\bar{H}$ atoms, the two-body H–$\bar{H}$ states of our interest may or may not necessarily be the lowest-energy state of the greater $(e^+e^-p\bar{p})$ system. Its relative position depends on the interatomic separation. We mentioned earlier that at large interatomic separations, the two-body state with separated atoms and leptons in the $1s$ orbitals is the lowest-energy state of the greater $(e^+e^-p\bar{p})$ four-body system. At small interatomic separations, the two-body molecular state of the H and $\bar{H}$ lies higher than the variational adiabatic lowest-energy state which is characterized by strong $e^+ - e^-$ correlations, and the two-body molecular state of the H and $\bar{H}$ is an excited state of the greater $(e^+e^-p\bar{p})$ system. It will be of great interest in future work to investigate how the two-body H–$\bar{H}$ state may preserve or otherwise mix their distinct molecular characteristics with the $e^+ - e^-$-correlated state, as the system dynamically traverses from large interatomic separations to the region of small separations.

To follow the four-body problem in the two-body atomic basis, we study the system from outside-in as the H and the $\bar{H}$ approach each other, and we examine their virtual excitations into excited H–$\bar{H}$ configurations, as the interatomic distance decreases. A good method to carry out such an investigation is to use the perturbation theory, having the atomic H and $\bar{H}$ as unperturbed composite particles, as in previous study of molecular states in heavy mesons in hadron physics.[11] The perturbation theory can be justified as an useful tool here because the composite H and $\bar{H}$ atoms are neutral objects, and their residue interaction V_I between the H and the $\bar{H}$ contains four terms (as given in Eq.(3) below) involving many cancellations due to the opposite charges of e^- and p of one atom on the one hand, and additional cancellations due to the opposite charges of the e^+ and $\bar{p}$ of the

other antiatom on the other hand. As a consequence, the residue interaction is small in magnitude. Using $V_{\rm I}/(\Delta E)$, where $V_{\rm I} = \boldsymbol{r}_a \cdot \boldsymbol{r}_b/r^3$ is the dipole–dipole interaction and ΔE is the energy denominator from the ground to the first excited state of the H atom, we roughly estimated $V_{\rm I}/\triangle E$ at interatomic separation $r = 3, 5$ and 8 a.u. to be $\sim$0.05, 0.01 and 0.003, respectively. Clearly, the next higher-order term involving the ratio $(V_{\rm I}/\triangle E)^2$ will be even smaller and the perturbation series is expected to converge. Therefore these numbers justify the application of the perturbation theory to the H–$\bar{\rm H}$ interaction potential in intermediate interatomic distances (i.e. $3 \leq r \leq 10$ a.u.).

Within the perturbation theory, the H–$\bar{\rm H}$ interaction potential, at present, is known only within the leading order.[12] It is positive for large distances, with a barrier whose peak lies in the region of short distances. It decreases precipitously at very short distances. Previous analysis of the next-to-leading order interaction potential between the H and the $\bar{\rm H}$ assumed an expansion of the energy denominator up to the first order of the state energies.[12] Such an expansion may not be accurate. It is of interest to re-evaluate more accurately this interaction potential, $V_{H\bar{H}}(r)$, up to the next-to-leading order (second order) in the residue interaction $V_{\rm I}$. We shall interest in the interaction potential for the elastic channel for which the initial incoming and the final outgoing H and $\bar{\rm H}$ atoms are in their respective ground states at asymptotic separations. The interaction potential for states with excited H and $\bar{\rm H}$ atoms at asymptotic separations can be similarly considered in a simple generalization.

For small interatomic distances, the $e^+ - e^-$ correlations become considerably important and we shall also study the additional $e^+ - e^-$ correlation effects on the potential energy around this region of separation. Needless to say, it is necessary in the future to include a greater number of the degrees of freedom, to take into account additional types of polarization of the two-body states. The perturbation theory results obtained here can provide a benchmark against which additional distortions may be measured. They can bring us to a better understanding of the scattering potential and the complexity of the spectrum that is associated with the four-body system.

This paper is organized as follows. In Section 2, we review the formulation of the four-body problem in terms of the interaction of two composite objects using separable two-body basis. In Section 3, we show how to evaluate the interaction matrix elements and the interaction potential. The results of the H–$\bar{\rm H}$ interaction potential and the examination of the stability with respect to $e^+ - e^-$ correlations are given in Sections 4 and 5, respectively. Finally, Section 6 gives some discussions and conclusions of the present work. Some of the details of the analytical formulae are presented in the Appendix. Atomic units $m = \hbar = e = 1$ are used throughout the paper unless otherwise indicated.

2. The four-body problem in a separable two-body basis

We shall review the formulation of the four-body problem in a separable two-body basis in terms of the interaction of two composite particles as presented previously.[11] As applied to the H–$\bar{\rm H}$ system, we choose the four-body coordinate system as shown in Fig.1 and label constituents p, e^-, e^+, and $\bar{p}$ as particles 1, 2, 3, and 4, respectively with a non-relativistic Hamiltonian

$$H = \sum_{j=1}^{4} \frac{\boldsymbol{p}_j^2}{2m_j} + \sum_{j=1}^{4}\sum_{k>j}^{4} V_{jk} + \sum_{j=1}^{4} m_j, \qquad (1)$$

in which particle j has a momentum $\boldsymbol{p}_j$ and a rest mass m_j. The pairwise interaction $V_{jk}(\boldsymbol{r}_{jk})$ between particle j and particle k depends on the relative coordinate between them, $\boldsymbol{r}_{jk} = \boldsymbol{r}_j - \boldsymbol{r}_k$. We introduce the two-body momentum $\boldsymbol{P}_{jk} = \boldsymbol{p}_j + \boldsymbol{p}_k$, and the two-body internal relative momentum $\boldsymbol{p}_{jk} = f_k\boldsymbol{p}_j - f_j\boldsymbol{p}_k$, where $f_k = m_k/m_{jk}$, $m_{jk} = m_j + m_k$. We partition the Hamiltonian so that in the lowest order the state in question can be described by a state of the unperturbed Hamiltonian. We choose to partition H into an unperturbed Hamiltonian $h_{12} + h_{34}$ of atoms $A(12)$ and $B(34)$ according to

$$H = \frac{\boldsymbol{P}_{12}^2}{2m_{12}} + \frac{\boldsymbol{P}_{34}^2}{2m_{34}} + V_{\rm I} + h_{12} + h_{34}, \qquad (2)$$

$$V_{\rm I} = V_{14}(\boldsymbol{r}_{14}) + V_{13}(\boldsymbol{r}_{13}) + V_{23}(\boldsymbol{r}_{23}) + V_{24}(\boldsymbol{r}_{24}), \qquad (3)$$

$$h_{jk} = \frac{\boldsymbol{p}_{jk}^2}{2\mu_{jk}} + V_{jk}(\boldsymbol{r}_j - \boldsymbol{r}_k) + m_{jk}$$

for

$$(jk) = A(12) \quad \text{and} \quad B(34), \qquad (4)$$

where $\mu_{jk} = m_j m_k/m_{jk}$. The eigenvalues of the Hamiltonians h_{12} and h_{34} can be solved separately

to obtain the bound state wavefunctions and masses $M_{jk}(\nu)$ of atoms A and B,

$$\begin{aligned} h_{jk}|(jk)_\nu\rangle &= [\epsilon_{jk}(\nu)+m_{jk}]|(jk)_\nu\rangle \\ &= M_{jk}(\nu)|(jk)_\nu\rangle. \end{aligned} \tag{5}$$

The four-body Hamiltonian becomes

$$H = \frac{\boldsymbol{P}_{12}^2}{2m_{12}} + \frac{\boldsymbol{P}_{34}^2}{2m_{34}} + V_{\rm I} + M_{12}(\nu) + M_{34}(\nu'). \tag{6}$$

The above non-relativistic approximation is obtained from relativistic results by neglecting terms of order ϵ_{jk}/M_{jk} and higher.[13] In order to satisfy the boundary condition at large separations for which $V_{\rm I}$ approaches zero, we need to include some of these higher-order terms and modify m_{12} and m_{34} in the above equation to $M_{12}(\nu)$ and $M_{34}(\nu')$ so that the Hamiltonian becomes

$$\begin{aligned} H \;=\; & \frac{\boldsymbol{P}_{12}^2}{2M_{12}(\nu)} + \frac{\boldsymbol{P}_{34}^2}{2M_{34}(\nu')} + V_{\rm I} \\ & + M_{12}(\nu) + M_{34}(\nu'). \end{aligned} \tag{7}$$

The above Hamiltonian then describes properly the asymptotic behaviour at large separations of the two atoms. This Hamiltonian H is related to the standard Hamiltonian

$$H_{\rm stand} = \frac{\boldsymbol{p}_e^2}{2m_e} + \frac{\boldsymbol{p}_{\rm e^+}^2}{2m_{\rm e^+}} + \sum_{j=1}^{4}\sum_{k>j}^{4} V_{jk} + \sum_{j=1}^{4} m_j, \tag{8}$$

by $H = H_{\rm stand} + \Delta$,

$$\begin{aligned} \Delta \;=\; & \frac{\boldsymbol{p}_p^2}{2m_p} + \frac{\boldsymbol{p}_{\bar p}^2}{2m_{\bar p}} + \boldsymbol{P}_{12}^2\left(\frac{1}{2M_{12}(\nu)} - \frac{1}{2m_{12}}\right) \\ & + \boldsymbol{P}_{34}^2\left(\frac{1}{2M_{34}(\nu')} - \frac{1}{2m_{34}}\right), \end{aligned} \tag{9}$$

and Δ is a small quantity which can be neglected in the Born–Oppenheimer limit of fixed baryon centres.

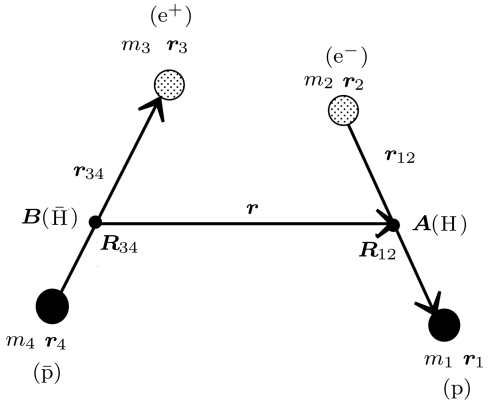


Fig.1. The coordinates of the $\{p, \mathrm{e}^-, \mathrm{e}^+,$ and $\bar{\mathrm{p}}\}$ system.

We consider a four-body system in which both atoms will be in their ground states $|A_0(12)B_0(34)\rangle$ at asymptotically large interatomic separations where the residue interactions $V_{\rm I}$ vanishes. When we include $V_{\rm I}$ as a perturbation, the eigenfunction of H becomes

$$\Psi(\boldsymbol{r},\boldsymbol{r}_{12},\boldsymbol{r}_{34}) = \psi(\boldsymbol{r})\left\{|A_0B_0\rangle + \sum_{\lambda,\lambda'}{}' \frac{|A_\lambda B_{\lambda'}\rangle\langle A_\lambda B_{\lambda'}|V_{\rm I}|A_0B_0\rangle}{\epsilon_A(\lambda)+\epsilon_B(\lambda')-\epsilon_A(0)-\epsilon_B(0)}\right\}, \tag{10}$$

where $\boldsymbol{r} = \boldsymbol{R}_{12} - \boldsymbol{R}_{34}$ is the interatomic separation (see Fig.1), $\boldsymbol{R}_{jk} = f_j\boldsymbol{r}_j + f_k\boldsymbol{r}_k$ is the centre-of-mass coordinate of m_j and m_k, and $\sum'_{\lambda\lambda'}$ indicates that the sum is over all atomic states, including continuum states, except $|A_0B_0\rangle$. The eigenvalue equation is

$$\begin{aligned} H\,\Psi(\boldsymbol{r},\boldsymbol{r}_{12},\boldsymbol{r}_{34}) \;=\; & [M_{12}(0)+M_{34}(0)+\epsilon] \\ & \times\Psi(\boldsymbol{r},\boldsymbol{r}_{12},\boldsymbol{r}_{34}). \end{aligned} \tag{11}$$

Working in the centre-of-mass frame and taking the scalar product of the above equation with $|A_0B_0\rangle$, we obtain the Schrödinger equation for the motion of $A_0(12)$ relative to $B_0(34)$,

$$\left\{\frac{\boldsymbol{p}^2}{2\mu_{AB}} + V(\boldsymbol{r})\right\}\psi(\boldsymbol{r}) = \epsilon\psi(\boldsymbol{r}), \tag{12}$$

where $\boldsymbol{p}$ is the relative momentum of the composite particles

$$\boldsymbol{p} = \frac{M_{34}(0)\boldsymbol{P}_{12} - M_{12}(0)\boldsymbol{P}_{34}}{M_{12}(0)+M_{34}(0)}, \tag{13}$$

and μ_{AB} is the reduced mass of the two atoms

$$\mu_{AB} = \frac{M_{12}(0)M_{34}(0)}{M_{12}(0)+M_{34}(0)}. \tag{14}$$

3. Evaluation of H and $\bar{\rm H}$ interaction matrix elements

The Schrödinger equation (12) involves the interatomic separation $\boldsymbol{r}$ and describes the motion between

two composite atoms. Because the mass of the proton is much greater than the mass of the electron and the positron, the interatomic separation $\boldsymbol{r}$ is approximately equal to the internuclear separation $\boldsymbol{r}_{14}$. The atom-atom potential $V(\boldsymbol{r})$ in Eq.(12) is given by

$$V(\boldsymbol{r}) = \langle A_0B_0|V_{\rm I}|A_0B_0\rangle - {\sum}'_{\lambda,\lambda'} \frac{|\langle A_\lambda B_{\lambda'}|V_{\rm I}|A_0B_0\rangle|^2}{\epsilon_A(\lambda)+\epsilon_B(\lambda')-\epsilon_A(0)-\epsilon_B(0)}, \tag{15}$$

where $|A_0B_0\rangle$ is a product of two 1s orbitals of the hydrogen and the antihydrogen. We label $V(\boldsymbol{r})$ as $V_{H\bar{H}}(r)$, and introduce $E(\boldsymbol{r}) = V(\boldsymbol{r}) - 1$. We call the first (leading-order) term on the right-hand side the direct potential, $V_{\rm dir}(\boldsymbol{r})$,

$$V_{\rm dir}(\boldsymbol{r}) = \langle A_0B_0|V_{\rm I}|A_0B_0\rangle, \tag{16}$$

and the second (next-to-leading order) term the polarization potential, $V_{\rm pol}(\boldsymbol{r})$,

$$V_{\rm pol}(\boldsymbol{r}) = -{\sum}'_{\lambda,\lambda'} \frac{|\langle A_\lambda B_{\lambda'}|V_{\rm I}|A_0B_0\rangle|^2}{\epsilon_A(\lambda)+\epsilon_B(\lambda')-\epsilon_A(0)-\epsilon_B(0)}. \tag{17}$$

The direct potential is given by the sum of the four matrix elements $\langle A_0B_0|V_{jk}(\boldsymbol{r}_{jk})|A_0B_0\rangle$ of Eq.(3). From the 1s wavefunctions we can analytically determine[12]

$$\langle A_0B_0|V_{\rm I}|A_0B_0\rangle = \frac{{\rm e}^{-2r}}{r}\left(-1-\frac{5}{8}r+\frac{3}{4}r^2+\frac{1}{6}r^3\right). \tag{18}$$

The polarization potential $V_{\rm pol}(r)$ is obtained as a double summation of λ and λ', representing the virtual excitation of the H and $\bar{\rm H}$ from 1s states to excited $\lambda-\lambda'$ atomic states. It contains contributions where $\lambda-\lambda'$ are bound–bound, bound–continuum (or vice versa), or continuum–continuum states.

For the evaluation of the bound–bound component of the polarization potential, $V_{\rm pol}^{\rm bb}(r)$, we shall use the Fourier transform method.[11,14] We represent the internal wavefunctions in $A_\lambda(12)$ and $B_{\lambda'}(34)$ by normalized eigenfunctions of the hydrogen atom $\phi_\lambda^A(\boldsymbol{r}_{12})$ and $\phi_{\lambda'}^B(\boldsymbol{r}_{34})$, respectively. The matrix elements $\langle A_\lambda B_{\lambda'}|V_{\rm I}|A_0B_0\rangle$ is then a sum of four terms with $V_{\rm I}$ given by Eq.(3). Each of these terms is given by

$$\langle A_\lambda B_{\lambda'}|V_{jk}(\boldsymbol{r}_{jk})|A_0B_0\rangle = \int \frac{{\rm d}\boldsymbol{p}}{(2\pi)^3}{\rm e}^{{\rm i}\boldsymbol{p}\cdot\boldsymbol{r}}\tilde{\rho}_{\lambda0}^A[f_A(jk)\boldsymbol{p}]\tilde{\rho}_{\lambda'0}^B[f_B(jk)\boldsymbol{p}]\tilde{v}_{jk}(\boldsymbol{p}), \tag{19}$$

where

$$\tilde{\rho}_{\lambda0}^{A,B}(\boldsymbol{p}) = \int {\rm d}\boldsymbol{y}{\rm e}^{{\rm i}\boldsymbol{p}\cdot\boldsymbol{y}}\rho_{\lambda0}^{A,B}(\boldsymbol{y}), \tag{20}$$

and

$$\tilde{v}_{jk}(\boldsymbol{p}) = \int {\rm d}\boldsymbol{r}_{jk}{\rm e}^{-{\rm i}\boldsymbol{p}\cdot\boldsymbol{r}_{jk}}V_{jk}(\boldsymbol{r}_{jk}), \tag{21}$$

with $\rho_{\lambda0}^A(\boldsymbol{r}_{12}) = \phi_\lambda^*(\boldsymbol{r}_{12})\phi_0(\boldsymbol{r}_{12})$, $\rho_{\lambda'0}^B(\boldsymbol{r}_{34}) = \phi_{\lambda'}^*(\boldsymbol{r}_{34})\phi_0(\boldsymbol{r}_{34})$, and $f_{\{A,B\}}(jk)$ are the coefficients of the linear relation

$$\boldsymbol{r}_{jk} = \boldsymbol{r} + f_A(jk)\ \boldsymbol{r}_{12} + f_B(jk)\ \boldsymbol{r}_{34}, \tag{22}$$

where the values of $f_{\{A,B\}}(jk)$ are given in Ref.[11].

To calculate the matrix element Eq.(19), we fix the vector $\boldsymbol{r}$ to lie along the z-axis, and quantize the azimuthal component of the magnetic quantum number m to be projections along the z-axis. We limit our consideration to intermediate states with $l = 1$ orbital angular momentum, as the dominant polarizing interaction is the dipole–dipole excitation. The bound–bound intermediate states are then $(\lambda,\lambda') = (\{n,(l=1),m\},\{n',(l=1),m'\})$ where n and n' are principal quantum numbers and $n,n' \geq 2$. The matrix element $\langle A_\lambda B_{\lambda'}|V_{jk}(\boldsymbol{r}_{jk})|A_0B_0\rangle$ is non-vanishing only for $\{\lambda = 1m;\lambda' = 1(-m)\}$ with $\{m = -1,0,1\}$, when both atoms are excited.

We write down the 1s and np hydrogen wavefunctions explicitly and obtain the Fourier transform of the transition density $\tilde{\rho}_{\lambda0}^{A,B}(\boldsymbol{p})$ (see Eq.(A8) in Appendix A)

$$\tilde{\rho}_{\lambda0}^{A,B}(\boldsymbol{p}) = \frac{(2\pi)^{3/2}N_{00}N_{n1}Y_{00}(\hat{r})}{(n+1)^2} \times \sum_{k=0}^{n-2}\binom{n+1}{k}\frac{\beta^{(n-2-k)}}{N'_{n1k}} \times (1-\beta)^k F_{n1k}\left(\frac{\boldsymbol{p}}{n+1}\right), \tag{23}$$

where $\beta = 1/(n+1)$,

$$N'_{n1k} = \sqrt{\left[\frac{2(n+1)}{n}\right]^3\frac{(n-2-k)!}{2(n-k)(n-k+1)!}}, \tag{24}$$

$$F_{n1k}\left(\frac{\boldsymbol{p}}{n+1}\right) = {\rm i}\sqrt{\frac{2}{\pi}\frac{(n-2-k)!}{(n+1)!}}\frac{2^4\ n^2}{\sqrt{n+1}} \times \left(\frac{\dfrac{np}{n+1}}{\left[\left(\dfrac{np}{n+1}\right)^2+1\right]^3}\right)\mathcal{C}_{n-2-k}^2$$

$$\times \left(\frac{\left(\frac{np}{n+1}\right)^2 - 1}{\left(\frac{np}{n+1}\right)^2 + 1} \right) Y_\lambda(\hat{p}), \quad (25)$$

and $\mathcal{C}_i^q(q)$ denotes the Gegenbauer polynomials.

Upon substituting the above Fourier transform of the transition density $\tilde{\rho}_{\lambda 0}^{A,B}(\boldsymbol{p})$ into Eq.(19), we can carry out the angular part of the integral analytically. We recognize

$$\mathrm{e}^{\mathrm{i}\boldsymbol{p}\cdot\boldsymbol{r}} = \sum_{l=0}^{\infty} (2l+1)\mathrm{i}^l j_l(pr) P_l(\cos\theta_p), \quad (26)$$

and we can easily carry out the angular integral by using

$$\int_0^{2\pi} \mathrm{d}\phi \int_{-1}^{1} \mathrm{d}\eta \; \mathrm{e}^{\mathrm{i}\boldsymbol{p}\cdot\boldsymbol{r}} \; Y_{1m}(\theta_p) Y_{1-m}(\theta_p) = \begin{cases} j_0(pr) - 2j_2(pr) & (\text{for} m = 0), \\ j_0(pr) + j_2(pr) & (\text{for} m{=}1), \end{cases} \quad (27)$$

where $j_l(x)$ and $P_l(z)$ are spherical Bessel function and Legendre polynomial of degree l, respectively. The remaining one-dimensional integral in the momentum space can be carried out numerically.

For the evaluation of the bound-continuum $V_{\mathrm{pol}}^{\mathrm{bc}}(r)$ and continuum–continuum $V_{\mathrm{pol}}^{\mathrm{cc}}(r)$ components of the polarization potential, we use the bound and continuum Coulomb wavefunctions in the configuration space[15] and perform a six-dimensional numerical integration involving the residue interaction V_{I} to obtain $\langle A_\lambda B_{\lambda'} | V_{\mathrm{I}} | A_0 B_0 \rangle$. The integrand is confined to a finite spatial region as the transition densities $\rho_{\lambda 0}^A(\boldsymbol{r}_{12})$ and $\rho_{\lambda 0}^B(\boldsymbol{r}_{34})$ contain the product of the continuum wavefunction and the ground state wavefunction. The sum over the continuum states can be carried out by discretizing the continuum spectrum which leads to converging results without much difficulty, as the magnitude of the matrix element decreases for continuum states with large momenta. We check our results against previous calculations of the C_6 dispersion-energy coefficient at large interatomic separations. Good agreement of the C_6 coefficient then allows us to proceed to explore the polarization potential at shorter interatomic separations.

4. The H and $\bar{\mathrm{H}}$ interaction potential

In the calculation to obtain the bound-bound contribution $V_{\mathrm{pol}}^{\mathrm{bb}}(r)$ to the polarization potential, we include all np states up to $n \leq n_{\max}$. Figure 2 shows the bound-bound results of $r^6 V_{\mathrm{pol}}^{\mathrm{bb}}(r)$ as a function of the interatomic separation r for different $n_{\max}$ number of bound states. Clearly, an increase in $n_{\max}$ for $n_{\max} > 10$ brings essentially little change in the shape but an overall small increase in the magnitude of the polarization potential, indicating that the result is sufficiently converged by considering up to $n \leq n_{\max} = 20$ states.

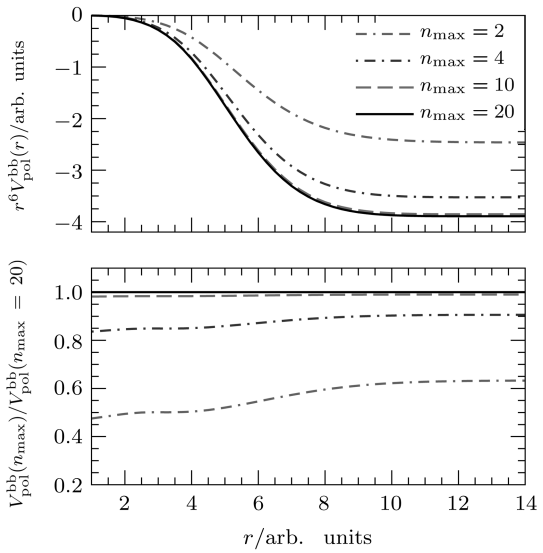


Fig.2. (a) Plot of $V_{\mathrm{pol}}^{\mathrm{bb}}(r) \times r^6$ as a function of the interatomic separation r for different $n_{\max}$ of $l = 1$ states. (b) Ratio of the summation from 2p up to $n_{\max}p$ states to the summation from 2p up to 20p states as a function of the interatomic separation r.

Results for the bound-bound, bound-continuum and continuum-continuum polarization potentials defined in Eq.(17) are presented in Fig.3 as a function of the interatomic separation r. To exhibit the asymptotic behaviour of $V_{\mathrm{pol}} \sim C_6/r^6$ at large r, the potentials are multiplied by r^6 in this figure. The numerical asymptotic values for each component are given in the parentheses, to be compared with the values obtained by Eisenschitz and London.[16] While $r^6 V_{\mathrm{pol}}^{\mathrm{bb}}(r)$ decreases monotonically as a function of r, the bound-continuum $r^6 V_{\mathrm{pol}}^{\mathrm{bc}}(r)$ and continuum-continuum $r^6 V_{\mathrm{pol}}^{\mathrm{cc}}(r)$ components have minima at $r \sim 6$ and $r \sim 4$ arb.units, respectively. The sum of all three contributions leads to $r^6 V_{\mathrm{pol}}(r)$ decreasing monotonically as a function of r. The result in Fig.3 also illustrates that the contribution of the continuum states to the polarization potential is substantial and cannot be neglected. The degree of the modification when continuum intermediate states are included at large r are also known from the perturbation calculation for

the C_6 coefficient of H_2 by Eisenschitz and London.[16] Note that the best C_6 coefficient has been known at least up to 8 digits of accuracy. Compare to the old calculation,[16] the present $C_6 = 6.498$ yields a better agreement to the modern $C_6 = 6.4990267$ dispersion-energy coefficient (i.e., less than ∼0.05%).

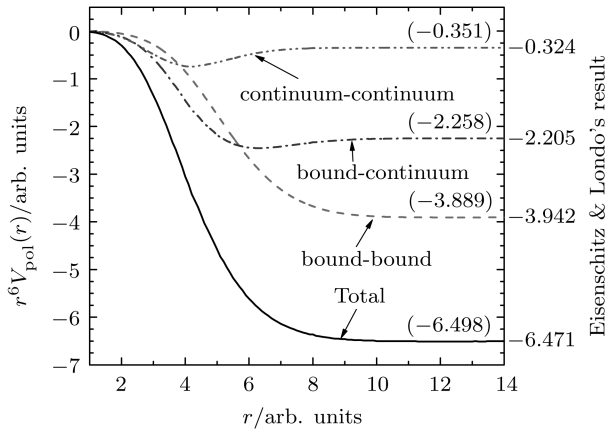


Fig.3. Bound-bound, bound-continuum and continuum-continuum components of the polarization potential multiplied by r^6 as a function of the interatomic separation r.

The functional form of the polarization potential $V_{\rm pol}(r)$ in Fig.4 implies that while the polarization potential varies as C_6/r^6 at large separations, they vary much more slowly as a function of r at small interatomic separations. This slow variation and the relatively flat behaviour can be seen from the total polarization potential $V_{\rm pol}(r)$ as a function of r shown as the dashed curve in Fig.4.

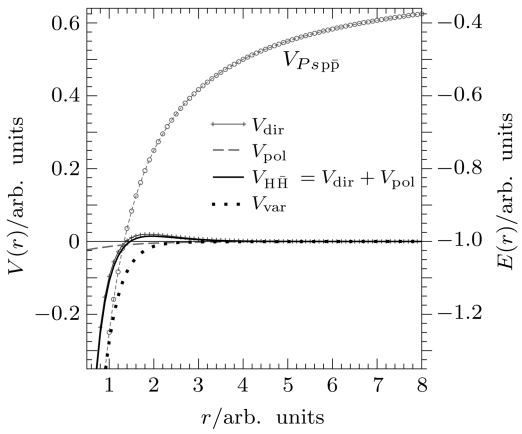


Fig.4. The H–$\bar{\rm H}$ interaction potential $V_{H\bar{H}}(r)$ and its components $V_{\rm dir}(r)$ and $V_{\rm pol}(r)$, as a function of the interatomic separation r. Shown here are also the potential $V_{Ps\,p\bar{p}}(r)$ for the $(e^+e^-)p\bar{p}$ configuration and the potential $V_{\rm var}(r)$ for the lowest-energy $(e^+e^-p\bar{p})$ four-body state obtained from the variational calculations of Ref.[8].

In the present calculation, we preserve the H and $\bar{\rm H}$ atomic identities and let them interact through $V_{\rm I}$ defined in Eq.(3). Within such a framework, the interatomic potential, $V_{\rm dir}$, $V_{\rm pol}$ and the total $V_{H\bar{H}}$ are shown as various curves in Fig.4. In Fig.4, the direct potential $V_{\rm dir}$ from Eq.(18) is slightly repulsive at large distances with a barrier whose peak lies in the region of small interatomic separations. It eventually decreases precipitously at smaller interatomic separations. The polarization potential $V_{\rm pol}(r)$ is, however, always attractive (Fig.3). The overall magnitude of the polarization potential is small because the residue interaction $V_{\rm I}$ consists of four terms which tend to cancel among themselves. The polarization potential provides a small overall modification of the interaction potential at short distances (Fig.4), but it changes the character of the interaction potential at intermediate separations of $r \sim$6 arb.units where the direct potential is small in magnitude, and the total interaction potential $V_{H\bar{H}}(r)$ exhibits a shallow local minimum at $r \sim$6 arb.units (Fig.5).

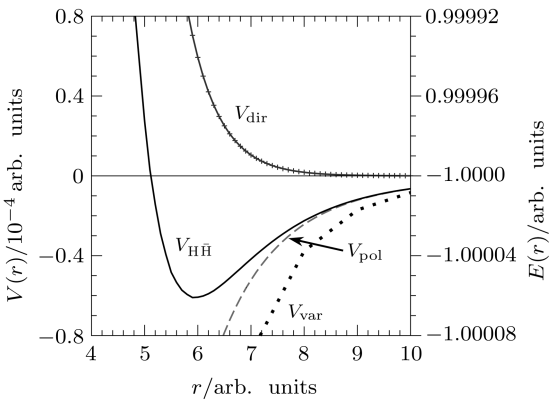


Fig.5. A magnified view of Fig.4 in the region of intermediate separations. Shown here are the H–$\bar{\rm H}$ interaction potential of $V_{H\bar{H}}(r)$ and its components $V_{\rm dir}(r)$ and $V_{\rm pol}(r)$, together with the potential $V_{\rm var}(r)$.[8]

To understand the rearrangement of the four particles in H and $\bar{\rm H}$, we also plot in Fig.4 the potential $V_{\rm var}(r)$ based on the variational calculation for the lowest-energy state of the greater $(e^+e^-p\bar{p})$ system.[8] Asymptotically, the variational potential $V_{\rm var}(r \to \infty)$ goes to zero in energy and almost coincides with $V_{H\bar{H}}(r)$ at large interatomic separations. At intermediate interatomic separations, the variational potential $V_{\rm var}(r)$ lies below $V_{H\bar{H}}(r)$. At very short distances (i.e. $r \lesssim$2 arb.units), $V_{\rm var}(r)$ decreases precipitously.

In Fig.5, we also present the potential

$$V_{Ps\,p\bar{p}}(r) = -\frac{1}{r_{14}} - 0.25 + 1 \qquad (28)$$

for the $Ps\mathrm{p}\bar{\mathrm{p}}$ configuration of a positronium and two heavy nuclei. Comparing $V_{\mathrm{var}}(r)$ with $V_{Ps\mathrm{p}\bar{\mathrm{p}}}(r)$ at large r, we find that the energy gap between them is 0.75 arb.units. Only when r is small and the two curves start to meet at $r \sim$1 arb.units will the rearrangement from H–$\bar{\mathrm{H}}$ to $Ps\mathrm{p}\bar{\mathrm{p}}$ becomes more probable. In the vicinity of the 'critical crossing-distance r_{c}' between the $V_{\mathrm{var}}(r)$ and the $V_{Ps\mathrm{p}\bar{\mathrm{p}}}(r)$ curves, the Born–Oppenheimer or adiabatic approximation starts to break down.[9,17] Nevertheless, in order to rearrange H–$\bar{\mathrm{H}}$ to become $Ps\mathrm{p}\bar{\mathrm{p}}$ as r decreases, some changes in the topology of the four-body system are certainly required. When r is slightly greater than 1 arb.units, the wavefunction may be regarded as a mixture of the two families of $H\bar{H}$ and $Ps\mathrm{p}\bar{\mathrm{p}}$. As the separation decreases further below $r <$ 1 arb.units, the $V_{Ps\mathrm{p}\bar{\mathrm{p}}}(r)$ and $V_{\mathrm{var}}(r)$ potential curves merge, indicating that the $Ps\mathrm{p}\bar{\mathrm{p}}$ with strong $\mathrm{e}^+ - \mathrm{e}^-$ correlations is the state of the lowest energy. The mixing of the two families at small interatomic separations and the strong $\mathrm{e}^+ - \mathrm{e}^-$ correlations for $r <$ 1 arb.units is in agreement with our analysis of stability against the variation of the $\mathrm{e}^+ - \mathrm{e}^-$ correlations in the next section.

In Fig.4, we show a magnified view of the interaction potential of H–$\bar{\mathrm{H}}$ for interatomic separations from 4 to 10 arb.units. In this region, the sum of the direct potential and the polarization potential gives rise to the H–$\bar{\mathrm{H}}$ interaction potential that possess a shallow local minimum located around $r \sim$6 arb.units and a barrier rising at $r \lesssim$5 arb.units. The depth of the well is found to be 6×10^{-5} arb.units or 1.63 meV.

It is easy to understand the formation of a potential 'pocket' for H–$\bar{\mathrm{H}}$. The system has the long-range attractive potential behaving as $\sim C_6/r^6$ at large r due to the polarization of the atoms as they approach each other. It experiences a repulsion at shorter distances arising from the repulsion of the e^- with the $\bar{p}$ and the e^+ with the p, which becomes effective at $1.5 < r <$ 5 arb.units. The combination of a long-range attraction and a shorter range repulsion results in a potential pocket at $r \sim$ 6 arb.units The interaction however turns to become attractive at smaller distances of $r \lesssim$1.5 arb.units due to the attraction of the leptons and the baryons.

Upon comparing with the variation potential $V_{\mathrm{var}}(r)$, we observe that $V_{H\bar{H}}(r)$ almost coincides with $V_{\mathrm{var}}(r)$ at the asymptotic region of large r. As r decreases, $V_{H\bar{H}}$ deviates from and lies above $V_{\mathrm{var}}(r)$ of the lowest-energy state, indicating that the state of the H–$\bar{\mathrm{H}}$ family is an excited state. At this point, we would like to point out that our aim here is to question, when there are no leptonic correlations in our trial wavefunctions, how the neutral H and $\bar{\mathrm{H}}$ interact at intermediate distances before they dissolve completely into positronium and protonium at shorter distances. Figure 5 provides the answer to our question.

5. Stability against variations in $\mathrm{e}^+ - \mathrm{e}^-$ correlations

Unlike the interaction between two hydrogen atoms, there is no exchange symmetry between the two leptons in the H–$\bar{\mathrm{H}}$ system. However, the correlation between the electron and the positron remains important in the electrostatic energy calculations. Therefore it is intriguing to see, within the present approach, when the $\mathrm{e}^+ - \mathrm{e}^-$ correlation can play an important role in the energy of the four-particle system. It is also crucial to find out whether the local minimum at $r \sim$6 arb.units examined in the last section is stable against $\mathrm{e}^+ - \mathrm{e}^-$ correlation perturbations. We therefore construct first a variational wavefunction with the variational parameter η that allows for $\mathrm{e}^+ - \mathrm{e}^-$ correlations,

$$\begin{aligned} &\Psi(\boldsymbol{r}, \boldsymbol{r}_{12}, \boldsymbol{r}_{34}, \boldsymbol{r}_{23}) \\ &= N_\eta \{ \sqrt{(1-\eta^2)} A_0(\boldsymbol{r}_{12}) B_0(\boldsymbol{r}_{34}) \\ &\quad + \eta C_0(\boldsymbol{r}_{23}) D_0(\boldsymbol{r}_{14}) \}, \end{aligned} \tag{29}$$

where N_η denotes the normalization constant such that for a fixed r

$$\int \mathrm{d}\boldsymbol{r}_{12} \mathrm{d}\boldsymbol{r}_{34} |\Psi(\boldsymbol{r}, \boldsymbol{r}_{12}, \boldsymbol{r}_{34}, \boldsymbol{r}_{23})|^2 = 1 \tag{30}$$

and

$$\int \mathrm{d}\boldsymbol{r}_{12} \mathrm{d}\boldsymbol{r}_{34} |C_0(\boldsymbol{r}_{23}) D_0(\boldsymbol{r}_{14})|^2 = 1. \tag{31}$$

The $C_0(\boldsymbol{r}_{23})$ is the ground-state positronium wavefunction centred at the centre of mass origin and $D_0(\boldsymbol{r}_{14})$ is a plane wave state in the continuum. We shall examine the case of $D_0(\boldsymbol{r}_{14})$ to be a state with zero momentum for p and $\bar{p}$ to be at rest, in the Born–Oppenheimer limit of fixed baryon centres, which supplies a constant to normalize the product wavefunction in Eq.(31). We numerically evaluate $\langle \Psi | H_{\mathrm{stand}}(r) | \Psi \rangle = E(r)$ as a six-dimensional integral in the configuration space.

Figure 6 gives the quantity $E(r) = V_{H\bar{H}}(r) - 1$ as a function of the variation parameter η for different interatomic separations r. For the largest values of

r in Fig.6(a), the minimum of $E(r)$ resides at $\eta = 0$, indicating that the $H\bar{H}$ system is stable against $e^+ - e^-$ correlations at large r. As r decreases, the $E(r)$ potential surface flattens as a function of η and the H–$\bar{\text{H}}$ system remains stable against $e^+ - e^-$ correlations. In the region where the energy minimum begins to shift away from $\eta = 0$, the variation of the energy as a function of η is shown for a finer increment of r in Fig.6(b). At $2.25 \geq r \geq 1.2$ arb.units, the minimum of $E(r)$ is shifted to a positive value of η. The equilibrium configuration is one in which the state is a mixture of the $H\bar{H}$ and the $Ps\text{p}\bar{\text{p}}$ configuration. The amplitude η at equilibrium increases as the interatomic separation decreases. As a result, the potential obtained from the variational method, $V_{\text{var}}(r)$, is lower than $V_{H\bar{H}}$ and $V_{Ps\text{p}\bar{\text{p}}}$ in this range of separation. At $r < 1.2$ arb.units, the lowest-energy state occurs at $\eta = \pm 1$ (Fig.6(a)) which corresponds to a state with a completely correlated $e^+ - e^-$ component $C_0(\boldsymbol{r}_{23})D_0(\boldsymbol{r}_{14})$ and the absence of the uncorrelated component $A_0(\boldsymbol{r}_{12})B_0(\boldsymbol{r}_{34})$. The equilibrium configuration resides in the $Ps\text{p}\bar{\text{p}}$ configuration, indicating the dominance of $e^+ - e^-$ correlation at small r. This picture is consistent with the findings of earlier variational calculations[5–9] and Fig.4.

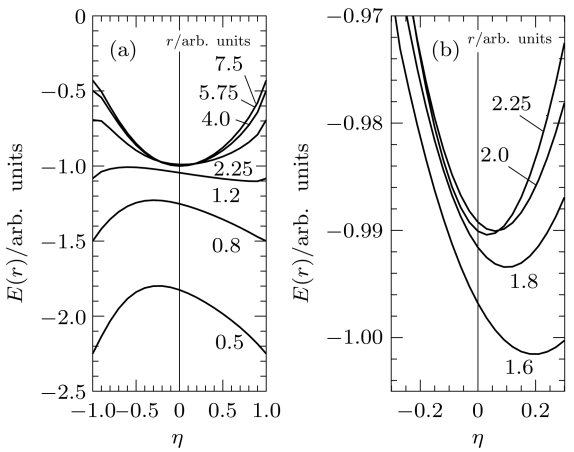


Fig.6. $E(r)$ as a function of η and the interatomic separation r.

While Fig.5 gives the general feature of the potential landscape with respect to $e^+ - e^-$ correlations as r changes, it is necessary to investigate whether the local potential minimum at $r = 6$ arb.units is stable against perturbations in $e^+ - e^-$ correlations. We replace $|A_0B_0\rangle$ in Eq.(29) by the wavefunction represented by the curly bracket of Eq.(10), with the $|A_\lambda B_{\lambda'}\rangle$ amplitudes evaluated at $r = 6$ arb.units and the summations over λ and λ' carried out to include all np states up to $n \leq n_{\max} = 20$. We find that at the location where $V_{H\bar{H}}(r) = E(r) + 1$ is a minimum in r, $E(r)$ is also a minimum with respect to variations in η at $\eta = 0$. We conclude that the local potential minimum of $V_{H\bar{H}}(r)$ at $r \sim 6$ arb.units is stable against perturbations from $e^+ - e^-$ correlations.

6. Discussions and conclusions

The four-body system of $(e^+e^-p\bar{p})$ contains a large degrees of freedom as the particles can appear in many different combinations and correlations, exemplified by the large number of parameters in an elaborate variational calculation. To be able to classify the states of the greater $(e^+e^-p\bar{p})$ system into simple families, if at all possible, will bring us to a better understanding of the complexity of the spectrum and the interactions that are associated with the complicated four-body problem.

In terms of the correlation between the e^+ and the e^-, one can perhaps roughly classify the greater $(e^+e^-p\bar{p})$ system as belonging to the H–$\bar{\text{H}}$ family without $e^+ - e^-$ correlations and the $Ps\text{p}\bar{\text{p}}$ family with strong $e^+ - e^-$ correlations. As one notes from energy considerations in Fig.4, the lowest-energy state of the $(e^+e^-p\bar{p})$ system is dominated by a state of the H–$\bar{\text{H}}$ family at large interatomic separations but at short distances the system is dominated by a state of the $Ps\text{p}\bar{\text{p}}$ family. The lowest-energy state therefore changes its character as the interatomic separation decreases.

In the collision of the H and the $\bar{\text{H}}$, the four-body system is prepared in the entrance channel of the H–$\bar{\text{H}}$ family as the composite particles approach each other. The system may follow the configuration of the lowest energy adiabatically in a slow collision, or it may follow the diabatic configuration of the H–$\bar{\text{H}}$ entrance channel when the collision is fast or when the intrinsic differences in the characteristics of the two configurations hindered their transition. In general, for the collision of arbitrary energies, it is necessary to couple the different channels explicitly and to follow the transition of the channels as the composite particles approach each other. We are therefore motivated to examine the interaction potential between the H and the $\bar{\text{H}}$ as composite particles, for which the e^- and the e^+ remain uncorrelated, orbiting around the p and $\bar{p}$ respectively.

We use the tool of the perturbation theory to ex-

amine this interaction potential, with the states of H and $\bar{\mathrm{H}}$ as unperturbed basis states. The perturbation theory can be an useful concept because the residue interaction V_{I} contains many cancellations and is small in magnitude compared to the value of typical energy denominators. The lowest-order perturbation theory gives an interaction potential $V_{\mathrm{dir}}(r)$ that is positive at large separations with a barrier located approximately between 1.4 to 5.0 arb.units and a precipitous drop at $r \lesssim 1.4$ arb.units. Our calculations have been carried out up to the next-to-leading order, by including virtual excitations of bound and continuum $l = 1$ states of the H and $\bar{\mathrm{H}}$ atoms. The next-to-leading order leads to the polarization potential that is always attractive. The bound-bound contribution to the polarization potential has been obtained by using the Fourier transform method involving the virtual excitation from the 1s states to all np states with $n \leq n_{\max} = 20$. The bound-continuum, and the continuum-continuum contributions have been obtained numerically by discretizing the continuum. The polarization potential results agree with previous calculations of the C_6 coefficient at large separations. The variation of the interatomic separation then allows us to obtain the polarization potential $V_{\mathrm{pol}}(r)$ at different separations.

We find that the interaction potential between the composite H and the $\bar{\mathrm{H}}$ possesses peculiar features. At intermediate distances, the total interaction potential $V_{H\bar{H}}(r)$, which is the sum of the direct potential $V_{\mathrm{dir}}(r)$ and the polarization potential $V_{\mathrm{pol}}(r)$, becomes negative. At shorter distances, the total potential shows a minimum at $r \sim 6$ arb.units, a barrier rising at $r \sim 5$ arb.units, and a broad barrier peak at $r \sim 1.9$ arb.units, as shown in Fig.4.

Our investigation on the stability against variations in the $\mathrm{e}^+ - \mathrm{e}^-$ correlation in Section 4 indicates that the composite system is stable against variations of the $\mathrm{e}^+ - \mathrm{e}^-$ correlation for $r \gtrsim 3$ arb.units but is unstable for $r \lesssim 3$ arb.units. Thus, the state with $\mathrm{e}^+ - \mathrm{e}^-$ correlations is the state of lowest energy at distances $r \lesssim 3$ arb.units, but the composite H–$\bar{\mathrm{H}}$ state may remain stable without substantial $\mathrm{e}^+ - \mathrm{e}^-$ correlations as an excited system for $r \gtrsim 3$ arb.units.

The shallow local minimum located around interatomic separations of $r \sim 6$ arb.units has a depth of 6×10^{-5} arb.units. One can use the interaction potential $V_{H\bar{H}}(r)$ and solve the Schrödinger equation (12) for the two-body H–$\bar{\mathrm{H}}$ states. It is necessary in the future to include a greater number of the degrees of freedom, to take into account additional types of polarization of the two-body states such as the virtual excitation of the d, f, ... states. As the residue interaction is dominated by the dipole-dipole interaction, the higher multipole interactions are expected to be diminishing in their importance and will not modify greatly the gross features of the interaction potential. Because the polarization potential is always negative, the addition of these multipole interactions will probably only deepen slightly the local potential minimum at $r \sim 6$ arb.units.

Returning to the question of channel coupling and reaction processes, we wish to emphasize that we have obtained only the interaction potential $V_{H\bar{H}}$ for the channel of the H and the $\bar{\mathrm{H}}$ as composite objects. We have in effect constructed the interaction potential only for one of the diabatic basis configurations. Interaction potentials for other basis configurations can be obtained in different analysis and a full picture of adiabatic or diabatic motion for reactions at an arbitrary energy needs to be investigated by a couple-channel analysis involving different diabatic channels with different interaction potentials and transition matrix elements.

In conclusion, we have examined the interaction potential of the H–$\bar{\mathrm{H}}$ system as composite objects using the second-order perturbation theory with mutual polarizing excitations of the atoms. We found that the interaction potential has a peculiar local minimum at $r \sim 6$ arb.units and a barrier rising at $r \lesssim 5$ arb.units. The potential energy minimum is found to be stable against perturbations of the $\mathrm{e}^+ - \mathrm{e}^-$ correlation. Further definitive studies on the nature of the interaction potential energy around this energy minimum and the interplay between the H–$\bar{\mathrm{H}}$ state and other states of different configurations will be of great experimental and theoretical interests.

Acknowledgments

The authors wish to thank Professors Cheng-Guang Bao, Wen-Ning Zhang, J. H. Macek, and S. Y. Ovchinnikov for helpful discussions.

Appendix A: Fourier transform of the transition density $\rho_{\lambda 0}^{A,B}(\boldsymbol{r})$

We here derive the expression for the Fourier transform of the transition density, $\tilde{\rho}_{\lambda 0}^{A,B}(\boldsymbol{p})$, which in-

volves the product of $1s$ and np wavefunctions. The hydrogen wavefunction is given by

$$\phi_{nlm}(\boldsymbol{r}) = N_{nl}\left(\frac{Z}{a_{\rm o}}\right)^{l}\left(\frac{2r}{n}\right)^{l}\exp\left(\frac{-2Zr}{2na_{\rm o}}\right) \times L^{2l+1}_{n-l-1}\left(\frac{2Zr}{na_{\rm o}}\right)Y_{lm}(\hat{r}), \quad \text{(A1)}$$

where N_{nl} is the normalization constant, $Y_{lm}(\hat{r})$ is the spherical harmonic and $L^{(\alpha)}_n(x)$ is the Laguerre polynomial. Setting $Z = 1$, l =1 and $a_{\rm o} = 1$, we have

$$\begin{aligned}\rho^{A,B}_{\lambda 0}(\boldsymbol{r}) &= \phi_{000}(\boldsymbol{r})\phi_{n1m}(\boldsymbol{r}) \\ &= N_{00}N_{n1}\left(\frac{2r}{n}\right)\mathrm{e}^{-r(n+1)/n} \\ &\quad\times L^{3}_{n-2}\left(\frac{2r}{n}\right)Y_{00}(\hat{r})Y_{lm}(\hat{r}). \quad \text{(A2)}\end{aligned}$$

From Ref.[15], we have

$$\begin{aligned}&L^{(\alpha)}_j(\beta x) \\ &= \sum_{k=0}^{j}\binom{j+\alpha}{k}\beta^{(j-k)}(1-\beta)^k L^{(\alpha)}_{j-k}(x). \quad \text{(A3)}\end{aligned}$$

Now by letting $r' = (n+1)r$ and writing

$$\begin{aligned}&f_{n1}(r') \\ &= \left(\frac{2r'}{n(n+1)}\right)\mathrm{e}^{-r'/n}L^{3}_{n-2}\left(\frac{2r'}{n(n+1)}\right), \quad \text{(A4)}\end{aligned}$$

we use Eq.(A3) with $j = n-2$, $\alpha = 3$, and $\beta = 1/(n+1)$, and we obtain

$$f_{n1k}(r') = \sum_{k=0}^{n-2}\binom{n+1}{k}\beta^{(n-2-k)}(1-\beta)^k\left(\frac{2r'}{n}\right) \times \mathrm{e}^{-r'/n}L^{3}_{n-2-k}\left(\frac{2r'}{n}\right). \quad \text{(A5)}$$

Therefore, the transition density $\rho^{A,B}_{\lambda 0}(\boldsymbol{r}')$ becomes

$$\rho^{A,B}_{\lambda 0}(\boldsymbol{r}') = \frac{N_{00}N_{n1}}{(n+1)}f_{n1k}(r')Y_{00}(\hat{r})Y_{1m}(\hat{r}). \quad \text{(A6)}$$

One can Fourier transform $\rho^{A,B}_{\lambda 0}(\boldsymbol{r}')$ by

$$\tilde{\rho}^{A,B}_{\lambda 0}(\boldsymbol{p}) = \frac{(2\pi)^{3/2}N_{00}N_{n1}Y_{00}(\hat{r})}{(n+1)}\tilde{g}^{A,B}_{\lambda 0}(\boldsymbol{p}), \quad \text{(A7)}$$

where

$$\begin{aligned}\tilde{g}^{A,B}_{\lambda 0}(\boldsymbol{p}) &= \frac{1}{(n+1)}\int \mathrm{d}\boldsymbol{r}'\exp\{\mathrm{i}\boldsymbol{p}\cdot\boldsymbol{r}'/(n+1)\} \\ &\quad\times f_{n1}(r')Y_{lm}(\hat{r}) \\ &= \frac{1}{(n+1)}\int \mathrm{d}\boldsymbol{r}'\mathrm{e}^{\mathrm{i}\boldsymbol{p}'\cdot\boldsymbol{r}'}N'_{n1k}f_{n1k}(r') \\ &\quad\times Y_{1m}(\hat{r})/N'_{n1k}, \quad \text{(A8)}\end{aligned}$$

with $\boldsymbol{p}' = \boldsymbol{p}/(n+1)$. By recognizing that the latter integrand is identical to 'p wavefunctions', without laborious mathematics and algebra, one can make use of the formula for the momentum space 'radial' wavefunction of hydrogen atom given in Bransden and Joachain[18] and cast the Fourier transform of the above $\rho^{A,B}_{\lambda 0}(\boldsymbol{r}')$ into the results of Eqs.(23)–(25).

References

[1] Amoretti M, Amsler C, Bazzano G, Bonomi G, Bouchta A, Bowe P, Carraro C, Cesar C L, Charlton M, Doser M, Filippini V, Fontana A, Fujiwara M C, Funakoshi R, Genova P, Hangst J S, Hayano R S, Jorgensen L V, Lagomarsino V, Landua R, Lindelöf D, Rizzini E Lodi, Macri M, Madsen N, Manuzio G, Marchesotti M, Montagna P, Pruys H, Regenfus C, Riedler P, Rotondi A, Rouleau G, Testera G, Variola A and Werf D P van der (ATHENA Collaboration) 2002 *Nature* **419** 456
Amoretti M, Amsler C, Bazzano G, Bonomi G, Bouchta A, Bowe P, Carraro C, Cesar C L, Charlton M, Doser M, Filippini V, Fontana A, Fujiwara M C, Funakoshi R, Genova P, Hangst J S, Hayano R S, Jorgensen L V, Lagomarsino V, Landua R, Lindelöf D, Rizzini E Lodi, Macri M, Madsen N, Manuzio G, Marchesotti M, Montagna P, Pruys H, Regenfus C, Riedler P, Rotondi A, Rouleau G, Testera G, Variola A and Werf D P van der 2004 *Phys. Lett.* B **578** 23

[2] Gabrielse G, Bowden N S, Oxley P, Speck A, Storry C H, Tan J N, Wessels M, Grzonka D, Oelert W, Schepers G, Sefzick T, Walz J, Pittner H, Hänsch T W, Hessels E A (ATRAP Collaboration) 2002 *Phys. Rev. Lett.* **89** 213401
Gabrielse G, Bowden N S, Oxley P, Speck A, Storry C H, Tan J N, Wessels M, Grzonka D, Oelert W, Schepers G, Sefzick T, Walz J, Pittner H, Hänsch T W and Hessels E A 2002 *Phys. Rev. Lett.* **89** 222401
Gabrielse G, Bowden N S, Oxley P, Speck A, Storry C H, Tan J N, Wessels M, Grzonka D, Oelert W, Schepers G, Sefzick T, Walz J, Pittner H, Hänsch T W and Hessels E A 2005 *Adv. Atom Mol. Opt. Phys.* **50** 155

[3] Wong C Y, Kerman A K, Satchler G R and MacKellar A D 1984 *Phys. Rev.* C **29** 574

[4] Zygelman B, Saenz A, Froelich P and Jonsell S 2004 *Phys. Rev.* A **69** 042715

[5] Kolos W, Morgan D L Jr, Schrader D M and Wolniewicz L 1975 *Phys. Rev.* A **11** 1792

[6] Armour E A G, Carr J M and Zeman V 1998 *J. Phys.* B **31** L679
Armour E A G and Zeman V 1999 *Int. J. Quantum Chem.* **74** 645
[7] Froelich P, Jonsell S, Saenz A, Zylgelman B and Dalgarno A A 2000 *Phys. Rev. Lett.* **84** 4577
[8] Strasburger K 2002 *J. Phys.* B **35** L435
[9] Labzowsky L, Sharipov V, Prozorov A, Plunien G and Soff G 2005 *Phys. Rev.* A **72** 022513
[10] Sharipov V, Labzowsky L and Plunien G 2006 *Phys. Rev.* A **73** 052503
Sharipov V, Labzowsky L and Plunien G 2006 *Phys. Rev. Lett* **97** 103005
[11] Wong C Y 2004 *Phys. Rev.* C **69** 055202
[12] Morgan D L and Hughes V W 1973 *Phys. Rev.* A **7** 1811
[13] Wong C Y and Crater H W 2001 *Phys. Rev.* C **63** 044907
[14] Satchler G R and Love W G 1979 *Phys. Rep.* **55** 183
Petrovich F 1975 *Nucl. Phys.* A **251** 143
[15] Abramowitz M and Stegun I A *Handbook of Mathematical Functions* (New York: Dover Publications Inc) p785
[16] Eisenschitz R and London F 1928 *Zeitschrift für Physik* **50** 24
London F 1929 *Nature* **17** 516
[17] Strasburger K 2004 *J. Phys.* B **37** 4483
[18] Bransden B H and Joachain C J 1992 *Physics of Atoms and Molecules* (London: Longman Scientific) p626